

## Article

# *Botrytis cinerea* G Protein $\beta$ Subunit Bcgb1 Controls Growth, Development and Virulence by Regulating cAMP Signaling and MAPK Signaling

Jiejing Tang, Mingde Wu , Jing Zhang, Guoqing Li  and Long Yang \* 

State Key Laboratory of Agricultural Microbiology and Hubei Key Laboratory of Plant Pathology, Huazhong Agricultural University, Wuhan 430070, China; tangjiejing@webmail.hzau.edu.cn (J.T.); mingde@mail.hzau.edu.cn (M.W.); zhangjing1007@mail.hzau.edu.cn (J.Z.); guoqingli@mail.hzau.edu.cn (G.L.)  
\* Correspondence: yanglong@mail.hzau.edu.cn

**Abstract:** *Botrytis cinerea* is a necrotrophic phytopathogenic fungus that causes gray mold disease in many crops. To better understand the role of G protein signaling in the development and virulence of this fungus, the G protein  $\beta$  subunit gene *Bcgb1* was knocked out in this study. The  $\Delta Bcgb1$  mutants showed reduced mycelial growth rate, but increased aerial hyphae and mycelial biomass, lack of conidiation, failed to form sclerotia, increased resistance to cell wall and oxidative stresses, delayed formation of infection cushions, and decreased virulence. Deletion of *Bcgb1* resulted in a significant reduction in the expression of several genes involved in cAMP signaling, and caused a notable increase in intracellular cAMP levels, suggesting that G protein  $\beta$  subunit Bcgb1 plays an important role in cAMP signaling. Furthermore, phosphorylation levels of MAP kinases (Bmp1 and Bmp3) were increased in the  $\Delta Bcgb1$  mutants. Yeast two-hybrid assays showed that Bcgb1 interacts with MAPK (Bmp1 and Bmp3) cascade proteins (BcSte11, BcBck1, BcMkk1, and BcSte50), and the Bmp1-regulated gene *Bcgas2* was up-regulated in the  $\Delta Bcgb1$  mutant. These results indicated that G $\beta$  protein Bcgb1 is involved in the MAPK signaling pathway in *B. cinerea*. In summary, our results revealed that G $\beta$  protein Bcgb1 controls development and virulence through both the cAMP and MAPK (Bmp1 and Bmp3) signaling pathways in *B. cinerea*.

**Keywords:** *Botrytis cinerea*; G $\beta$  subunit; cAMP signaling pathway; MAPK signaling pathway



**Citation:** Tang, J.; Wu, M.; Zhang, J.; Li, G.; Yang, L. *Botrytis cinerea* G Protein  $\beta$  Subunit Bcgb1 Controls Growth, Development and Virulence by Regulating cAMP Signaling and MAPK Signaling. *J. Fungi* **2021**, *7*, 431. <https://doi.org/10.3390/jof7060431>

Academic Editor: Ulrich Kück

Received: 29 April 2021

Accepted: 27 May 2021

Published: 29 May 2021

**Publisher's Note:** MDPI stays neutral with regard to jurisdictional claims in published maps and institutional affiliations.



**Copyright:** © 2021 by the authors. Licensee MDPI, Basel, Switzerland. This article is an open access article distributed under the terms and conditions of the Creative Commons Attribution (CC BY) license (<https://creativecommons.org/licenses/by/4.0/>).

## 1. Introduction

*Botrytis cinerea* is an important phytopathogenic fungus and the causal agent of gray mold disease in more than 1400 plant species. It is responsible for significant economic losses in many important vegetables, fruits, and ornamentals [1]. The cost of controlling gray mold disease in the world has been estimated at over €1 billion per year. Due to its scientific and economic importance, *B. cinerea* is considered as the second most important fungal pathogen and the necrotrophic model fungus [2]. In the life cycle of *B. cinerea*, there are four different structures, including conidia, mycelia, sclerotia, and ascospores. Since sexual ascospores rarely occur in nature, the main source of the initial inoculum in the field is asexual conidia that formed from germinating sclerotia or hyphae, or survived in the last season [3]. Sclerotia are the melanized dormancy structures that can survive in adverse environment. When favorable conditions appear in spring, sclerotia will germinate to produce hyphae and conidia as the source of initial infection. Therefore, sclerotia and conidia play pivotal roles in the epidemic and life cycle of *B. cinerea* [3].

Heterotrimeric G proteins, which consist of G $\alpha$ , G $\beta$ , and G $\gamma$  subunits, transmit a variety of extracellular signals received by membrane-spanning G protein coupled receptors (GPCR) to intracellular effectors of eukaryotic cells [4]. When GPCR senses external signal stimulation, it triggers GDP-GTP exchange in G $\alpha$ , leading to the dissociation of G protein complex as

G $\alpha$ -GTP and G $\beta\gamma$  dimer. Both G $\alpha$ -GTP and G $\beta\gamma$  dimer can activate and regulate downstream signaling pathways, such as the cAMP and MAP kinase pathways [4,5].

In filamentous fungi, G proteins have been demonstrated to be required for growth, differentiation, mating, sporulation, and pathogenesis [4]. Like most characterized filamentous fungi, the plant pathogen *Magnaporthe oryzae* contains three G $\alpha$  subunit genes (*magA*, *magB*, and *magC*); one G $\beta$  subunit gene, *mgb1*; and one G $\gamma$  subunit gene, *MGG1*. Three G $\alpha$  subunit genes are involved in *M. oryzae* mating, but only *magB* (group I), like *mgb1* and *MGG1*, is required for appressorium formation and virulence [6–8]. In the soilborne vascular wilt fungus *Fusarium oxysporum*, deletion mutants of the G $\alpha$  subunit *Fga1* (group I) and the G $\beta$  subunit *Fgb1* displayed the similar phenotypes, i.e., altered colony morphology, reduced virulence and conidiation, and increased heat resistance [9,10]. However, deletion of the group III G $\alpha$  subunit *Fga2* results in some phenotypes different than those of *Fga1* and *Fgb1* mutants, such as complete loss of pathogenicity, no alteration on colony morphology, and conidiation [11]. Mutants lacking *Fga1* or *Fgb1* exhibit reduced intercellular cAMP levels, suggesting that G $\alpha$  subunit *Fga1* and G $\beta$  subunit *Fgb1* are involved in the cAMP signaling pathway [9,10]. In another soilborne vascular wilt fungus, *Verticillium dahliae*, the G $\beta$  subunit gene *VGB* positively regulates virulence and negatively regulates conidiation and microsclerotia formation [12].

In *B. cinerea*, the function of three G $\alpha$  subunit genes (*Bcg1*, *Bcg2*, and *Bcg3*) has been demonstrated by targeted gene deletion, suggesting that all of them are involved in the infection process. The *Bcg1* deletion mutants show altered colony morphology and significantly reduced virulence [13,14]. In contrast, deletion of *Bcg2* only results in a slight decrease in pathogenicity [13]. The third G $\alpha$  subunit, *Bcg3*, is important for conidiation, conidial germination, and virulence [15].  $\Delta Bcg1$  and  $\Delta Bcg3$  mutants show reduced intercellular cAMP levels and their defects are partially restored by exogenous cAMP, implying that *Bcg1* and *Bcg3* are the upstream components of cAMP signaling pathways. Although the G $\alpha$  subunits of *B. cinerea* have been investigated comprehensively, the functional role of the G $\beta$  subunit in growth, conidiation, sclerotia formation, and pathogenicity, as well as its downstream signaling pathway in *B. cinerea*, is still unclear.

In this study, we knocked out the G $\beta$  subunit gene *Bcgb1* using the split-marker strategy. The  $\Delta Bcgb1$  mutants exhibited defects in mycelial growth, conidiation, sclerotia formation, and virulence. Deletion of *Bcgb1* affected intracellular cAMP levels and the phosphorylation level of MAP kinases (*Bmp1* and *Bmp3*). Yeast two-hybrid assays showed that *Bcgb1* directly interacts with *Bmp1* upstream kinase *BcSte11*, *Bmp3* upstream kinases *BcBck1* and *BcMkk1*, and the *BcSte11/BcSte7/Bmp1* MAP kinase adaptor protein *BcSte50*. Moreover, the qRT-PCR result showed that *Bcgs2*, the downstream target gene of *Bmp1* [16], was remarkably up-regulated in  $\Delta Bcgb1$ . These results suggest that G $\beta$  protein *Bcgb1* is involved in regulation of the development and virulence via both cAMP signaling and MAPK (*Bmp1* and *Bmp3*) signaling in *B. cinerea*.

## 2. Materials and Methods

### 2.1. Fungal Strains and Culture Conditions

The wild-type strain B05.10 and its derived strains, including *Bcgb1* gene knockout mutants ( $\Delta Bcgb1$ -8,  $\Delta Bcgb1$ -43, and  $\Delta Bcgb1$ -64), were cultivated on potato dextrose agar (PDA) [17] at 20 °C. The *Bcgb1* gene knockout mutants were maintained on PDA amended with 100  $\mu\text{g}\cdot\text{mL}^{-1}$  hygromycin B (Calbiochem, San Diego, CA, USA). For growth experiments, the mutants and B05.10 were grown on PDA at 20 °C. Each plate was inoculated with a 5 mm-diameter mycelial agar plug taken from the edge of a 2-day-old colony. To characterize the growth rate, sclerotia formation, and infection cushion formation, a different strain was cultured in constant darkness. To characterize the sporulation, strains were grown under a 12 h light/dark cycle. To test the mycelial biomass, 10 mycelial plugs (5 mm) of each strain were inoculated into an Erlenmeyer flask (250 mL) containing 100 mL potato dextrose broth (PDB) [17], with three flasks for each strain, and the flasks were shake-incubated at 20 °C and 150 rpm for 2 days. Mycelial biomass of each strain was harvested

by paper-filtering, dried at 55 °C for 12 h, and weighed. To evaluate the response of *Bcgb1* knockout mutants to abiotic stress, the wild-type strain and *Bcgb1* knockout mutants were cultured on PDA medium amended with 1 M NaCl, 1 M KCl, 1 M sucrose, 1 M sorbitol, 0.1 mg/mL SDS, 0.3 mg/mL Congo Red (CR), 0.2 mg/mL CalcoFluor White (CFW), and 5mM H<sub>2</sub>O<sub>2</sub>. The colony diameters were measured at 72 h to calculate the relative mycelial growth rate of each strain. Each experiment was repeated three times.

## 2.2. Disruption of *Bcgb1*

The *Bcgb1* gene was disrupted using the split marker method [18]. The disruption strategy for *Bcgb1* is showed in Figure S1. The 5' and 3' flanking sequences of *Bcgb1* were amplified with the primers listed in Table S1 and then fused with part of the hygromycin fragment. Two split-marker DNA fragments were transformed into protoplasts of the WT strain B05.10 using the PEG-mediated transformed technique [19]. The hyphal tips of the deletion transformants were screened on PDA plates containing hygromycin B (100 µg mL<sup>-1</sup>) three times and verified by PCR. Single spore isolation was performed to obtain the homokaryotic deletion mutants. Three *Bcgb1* deletion mutants,  $\Delta Bcgb1-8$ ,  $\Delta Bcgb1-43$ , and  $\Delta Bcgb1-64$ , were further confirmed by Southern blot analysis using the right flank of the *Bcgb1* gene as a probe. Southern blot analysis was performed by the Gene Images™ AlkPhos Direct™ labeling and detection kit from GE Healthcare (Amersham Biosciences, Buckinghamshire, UK).

## 2.3. Extraction of DNA and RNA

Strains of *B. cinerea* were grown on PDA medium at 20 °C under darkness for 2 days. Genomic DNA of *B. cinerea* was extracted from the mycelia using the CTAB method [20]. Total RNA was extracted from mycelium samples of *B. cinerea* using the RNAiso Plus reagent (TaKaRa, Dalian, China) according to the manufacturer's instructions.

## 2.4. Pathogenicity and Penetration Assays

A pathogenicity test was performed with 5-week-old tobacco (*Nicotiana benthamiana*) leaves using 5 mm mycelial plugs from wild-type,  $\Delta Bcgb1-8$ , and  $\Delta Bcgb1-43$  mutant strains grown on PDA. Infected leaves were incubated at 20 °C under darkness with 100% relative humidity. The lesion diameters were measured at 72 h post inoculation.

Infection cushions were observed on onion epidermis as per a previous study [21]. Mycelial plugs (5 mm) of each strain were inoculated on onion epidermis and incubated at 20 °C under darkness. The epidermis was sampled and then stained with cotton blue before microscopic examination at 12 h and 24 h post inoculation, respectively. Each experiment was repeated three times.

## 2.5. Quantification of Intracellular cAMP

Mycelia were harvested from two-day-old PDB [17] liquid cultures, frozen in liquid nitrogen, and lyophilized for 20 h. For every 10 mg of lyophilized mycelium, 1 mL of 0.1 M HCl was added. Samples were centrifuged at 12,000 rpm for 15 min. The supernatant was used to determine cAMP concentration via the Monoclonal Anti-cAMP Antibody Based Direct cAMP ELISA Kit (NewEast Biosciences, Malvern, PA, USA) following the manufacturer's instructions.

## 2.6. Reverse Transcription and Fluorescence Quantitative PCR (RT-qPCR)

The cDNA was synthesized via the PrimeScript™ RT reagent kit (TaKaRa, Dalian, China) according to instructions from the manufacturer. An RT-qPCR was carried out in a CFX96 real-time PCR system (Bio-Rad, Hercules, CA, USA) with TB Green® Premix Ex Taq™ (Tli RNaseH Plus) (TaKaRa, Dalian, China). The *B. cinerea* actin gene *BcactA* (*Bcin16g02020*) was used as internal control. The relative expression of each gene was evaluated using the  $\Delta\Delta CT$  method [22]. All primers used for the RT-qPCR analyses are listed in Table S1. The RT-qPCR assay was repeated three times, each with three biological replicates.

### 2.7. Assays for Bmp1 and Bmp3 Phosphorylation

Total proteins were isolated from two-day-old mycelia with the protein lysis buffer (50 mM Tris-HCl, pH 7.4, 150 mM NaCl, 1 mM EDTA, 1% Triton X-100) containing 1% each of protease inhibitor cocktail, phosphatase inhibitor cocktail 2, and phosphatase inhibitor cocktail 3 (Sigma-Adrich, St. Louis, MO, USA) as previously described [23]. Then, the total proteins were separated by 10% SDS-PAGE and then transferred to PVDF (polyvinylidene difluoride) membranes (Bio-Rad, Hercules, CA, USA). Phosphorylation of the Bmp1 and Bmp3 MAP kinases was detected by using the phospho-p44/42 MAPK antibody (Cell Signaling Technology, Boston, MA, USA). The total Bmp1 and Bmp3 was detected with anti-MAPK ERK 1/2 antibody (Santa Cruz Biotechnology, Dallas, TX, USA). The anti-GAPDH was used as a loading control.

### 2.8. Yeast Two-Hybrid Assays

The Matchmaker™ Gold yeast two-hybrid system (Clontech, Mountain View, CA, USA) was used to analyze the protein–protein interactions. The full-length cDNA of *Bcgb1* (*Bcin08g01420*) was cloned into pGADT7 vector. Full-length cDNAs of *BcSte11* (*Bcin03g02630*), *BcSte7* (*Bcin04g05630*), *BcBck1* (*Bcin02g06590*), *BcMkk1* (*Bcin03g07190*), and *BcSte50* (*Bcin08g03660*) were cloned into pGBKT7 vector. A pair of plasmids (pGBKT7-53 and pGADT7-T) served as a positive control and a pair of plasmids (pGBKT7-Lam and pGADT7-T) was used as a negative control. The resulting prey and bait constructs were co-transformed in pairs into yeast strain Y2H following the manufacturer's instructions. Transformants were grown on SD-Leu-Trp at 30 °C for 3 days, and then transferred to SD-His-Leu-Trp. The resulting yeast cells were further tested for  $\beta$ -galactosidase activities. The primers used in this experiment are listed in Table S1.

## 3. Results

### 3.1. Identification and Deletion of the *Bcgb1* Gene in *B. cinerea*

The *Bcgb1* gene (*Bcin08g01420*) encoded a conserved G $\beta$  subunit protein. The *Bcgb1* protein (358 amino acids) contained a 7-WD40 repeat domain and shared high amino acid sequence identity with G $\beta$  proteins in *Aspergillus nidulans* (82.12%), *Neurospora crassa* (88.83%), *Ustilago maydis* (67.6%), *Rattus norvegicus* (64.53%), *Cryphonectria parasitica* (88.58%), *F. oxysporum* (89.69%), *V. dahliae* VGB (88.86%), and *M. oryzae* (88.86%), although had only 37.5% identity with the G $\beta$  subunit *gpb1* in *Schizosaccharomyces pombe* (Figure 1A). Moreover, phylogenetic analysis also showed that *Bcgb1* belonged to the same cluster as the G $\beta$  proteins previously reported using G $\alpha$  proteins as the outgroup (Figure 1C). Among the known G $\beta$  protein in the Protein Data Bank (PDB), the crystal structure of *Bcgb1* was predicted by using *R. norvegicus* G $\beta$  protein (PDB: 7cfm.1.B) as a template (Figure 1B).

To investigate the function of *Bcgb1*, a  $\Delta$ *Bcgb1* knockout mutant was generated by replacing the *Bcgb1* gene with a hygromycin-resistance cassette (HPT) (Figure S1A). After PEG-mediated transformation, three  $\Delta$ *Bcgb1* mutants ( $\Delta$ *Bcgb1*-8,  $\Delta$ *Bcgb1*-43, and  $\Delta$ *Bcgb1*-64) were obtained through PCR verification (Figure S1B) and further confirmed by Southern blotting analysis (Figure S1C).

### 3.2. *Bcgb1* Is Required for Hyphal Growth, Conidiation, Sclerotia Formation

To determine the role of *Bcgb1* in hyphal growth, conidiation, and sclerotia formation, two  $\Delta$ *Bcgb1* mutants ( $\Delta$ *Bcgb1*-8 and  $\Delta$ *Bcgb1*-43) grown on PDA were compared with the wild-type strain B05.10. Colonies of  $\Delta$ *Bcgb1* mutants showed a fluffy, dense aspect; a decreased colony diameter; and dramatically increased aerial hyphae compared to the wild type (Figure 2A,B). Microscopic analysis showed that the  $\Delta$ *Bcgb1* mutants produced more branches at the tip of the hyphae than that of the wild type (Figure 2A). After 15 days of incubation on PDA, the wild-type strain produced a large number of conidia and formed sclerotia. However, the  $\Delta$ *Bcgb1* mutants were unable to produce conidia and sclerotia (Figure 2A). In comparison with the wild type, the mycelial growth rate of the  $\Delta$ *Bcgb1* mutants was significantly reduced (Figure 2C), but the mycelial biomass was increased

(Figure 2D). These results indicate that Bcgb1 plays an important role in hyphal growth, conidiation, and sclerotia formation.

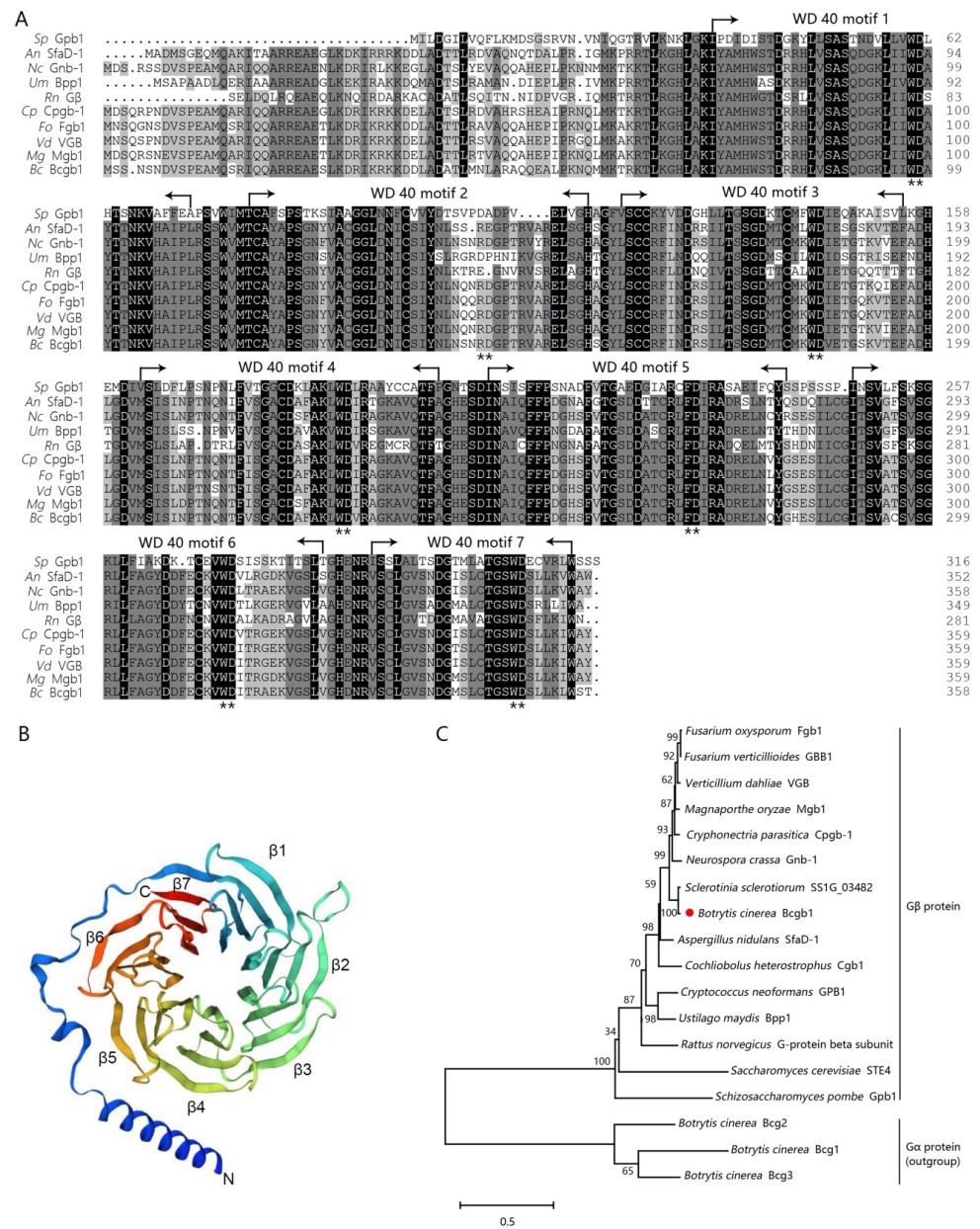


**Figure 1.** Sequence analysis of Bcgb1 in *B. cinerea*. **(A)** Amino sequence alignment of Bcgb1 orthologues. All conserved residues are shown in black and similar residues in grey. The positions of the seven WD repeats are labeled and indicated by arrows. \*\* means the conserved WD residues in WD repeats. **(B)** The crystal model of Bcgb1. The Gβ protein of *R. norvegicus* Gβ (PDB: 7cfm.1.B) was used as the template for the Bcgb1 model at the SWISS-MODEL website. The seven β-propeller blades were numbered. **(C)** A neighbor-joining tree based on amino acid sequences of Gβ protein in fungi. The following protein sequences were used: XP\_018249805 (fgb1), ABE67098 (GGB1), XP\_028497849 (VGB), BAC01165 (mgb1), XP\_009851210 (gnb-1), XP\_024550185 (Bcgb1), XP\_001595393 (SS1G\_03482), XP\_024345016 (SfaD), XP\_657685 (sfaD-1), AAO25585 (cgb1), AAD03596 (GPB1), XP\_011386498 (bpp1), 5TDH\_B (*R. norvegicus* Gβ protein), NP\_014855 (STE4), AAC37501 (gpb1), XP\_024548939 (Bcg1), XP\_024552854 (Bcg2), and XP\_024553380 (Bcg3). Bootstrap values (%) from 1000 replicates of the data are indicated above the nodes. The red dot represents the Gβ protein Bcgb1 of *B. cinerea* in this study.

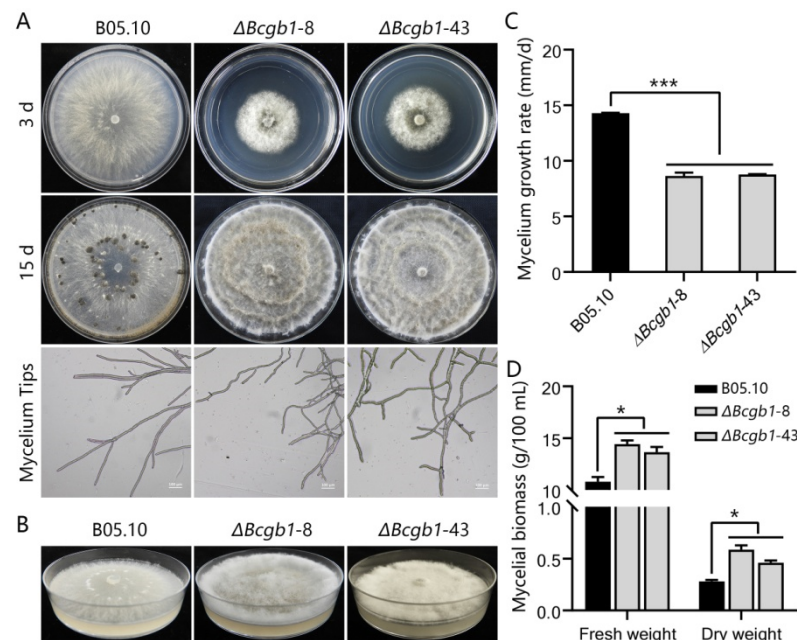


**Figure 2.** Bcgb1 is required for mycelial growth, conidiation, and sclerotia formation. (A) Colony morphology (3 d and 15 d) and mycelium tips (48 h) of the indicated strains cultured on PDA at 20 °C. (B) Aerial hyphae growth is increased in the  $\Delta Bcgb1$  mutants after incubation on PDA for 7 days at 20 °C. (C) Mycelial growth rate of the indicated strains cultured on PDA at 20 °C \*\*\*  $p < 0.001$ . (D) Mycelial biomass of the indicated strains cultured in PDB at 20 °C for 2 d. \*  $p < 0.05$ .

### 3.3. Bcgb1 Is Involved in Response to Cell Wall and Oxidative Stresses

To investigate functions of Bcgb1 in cell-wall integrity, we examined the sensitivity of the  $\Delta Bcgb1$  mutants to osmotic stress agents NaCl, KCl, sucrose, and sorbitol; cell-wall disturbing agents SDS, CR, and CFW; and oxidative stress  $H_2O_2$ . Our results show that there was no significant difference in relative growth rate between the  $\Delta Bcgb1$  mutants and wild type when cultured on PDA containing NaCl, KCl, sucrose, sorbitol, and CR (Figure 3). However, the relative growth rate of the  $\Delta Bcgb1$  mutants significantly increased when cultured on PDA containing SDS, CFW, and  $H_2O_2$  (Figure 3A,B). These results indicate that Bcgb1 plays a role in response to cell-wall and oxidative stresses.

### 3.4. Bcgb1 Is Important for Virulence in *B. cinerea*

To analyze the role of Bcgb1 in pathogenicity, unwounded and wounded tobacco leaves were inoculated with the mycelial agar plugs of  $\Delta Bcgb1$  mutants. The  $\Delta Bcgb1$  mutants showed significantly reduced virulence in tobacco leaves (Figure 4A). At 72 hpi, the lesion size of  $\Delta Bcgb1$  mutants on both unwounded and wounded leaves decreased by more than 50% compared with that of the wild type (Figure 4B). To determine the virulence defects of  $\Delta Bcgb1$  mutants in detail, we performed a penetration assay on onion epidermis. As shown in Figure 4C, the wild-type strain formed numerous infection cushions and successfully penetrated onion cells at 12 hpi and 24 hpi. However, the average number of infection cushions of  $\Delta Bcgb1$  mutants was much less than that of the wild type (Figure 4D). This revealed that the  $\Delta Bcgb1$  mutants delayed the formation of infection cushions to penetrate plant cells, resulting in the decrease of virulence. These results show that Bcgb1 is important for infection cushion formation and virulence.

### 3.5. Bcgb1 Is Involved in the Regulation of Intracellular cAMP Levels

To test whether deletion of Bcgb1 affects the cAMP levels in *B. cinerea*, the intracellular cAMP levels were measured in the hyphae stage of the  $\Delta Bcgb1$  mutants and wild type. The cAMP levels of two  $\Delta Bcgb1$  mutants were drastically increased about fourfold and sixfold, respectively, compared to the wild type (Figure 5A).

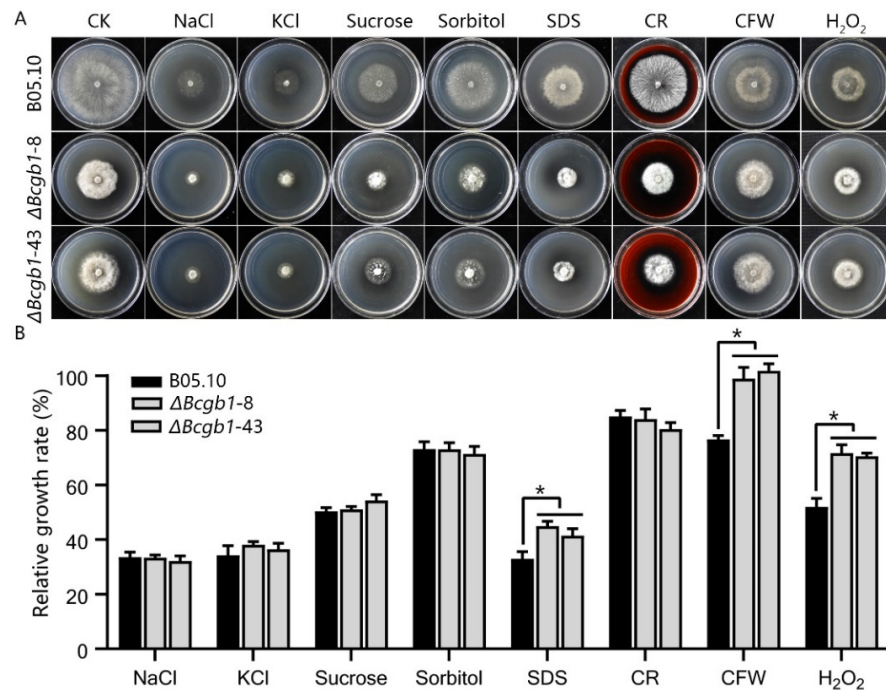


**Figure 3.** *Bcgb1* is involved in responses to cell-wall and oxidative stresses. **(A)** Sensitivity test of strains to salt stress (NaCl or KCl), osmotic stress (sucrose or sorbitol), cell-wall stress (SDS, CR, or CFW), and oxidative stress (H<sub>2</sub>O<sub>2</sub>). Strains were incubated on PDA supplemented with 1 M NaCl, 1 M KCl, 1 M sucrose, 1 M sorbitol, 0.1 mg/mL SDS, 0.3 mg/mL CR, 0.2 mg/mL CFW, and 5 mM H<sub>2</sub>O<sub>2</sub> at 20 °C for 72 h. **(B)** The relative mycelial growth rate of the indicated strains in the presence of various stresses. \* *p* < 0.05.

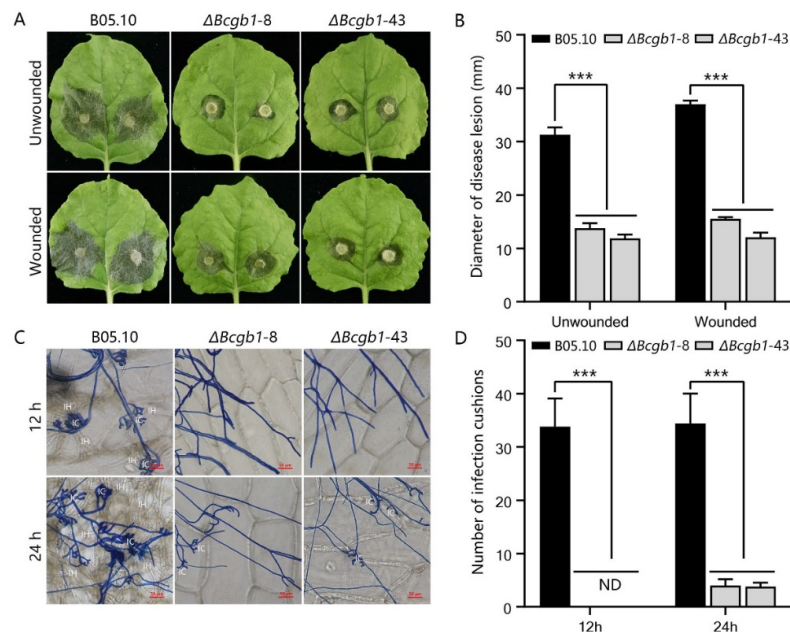


**Figure 4.** *Bcgb1* is important for virulence in *B. cinerea*. **(A)** Pathogenicity test of the indicated strains on unwounded and wounded tobacco leaves. Disease symptoms were photographed at 72 h post inoculation (20 °C). **(B)** Lesion size caused by the indicated strains in A. **(C)** Infection cushion formation by mycelium plugs of the indicated strains on onion epidermis at 12 h or 24 h post inoculation (20 °C). IC: infection cushion, IH: infectious hyphae. **(D)** Quantitative analysis of infection cushions of the indicated strains in C. \*\*\* *p* < 0.001.

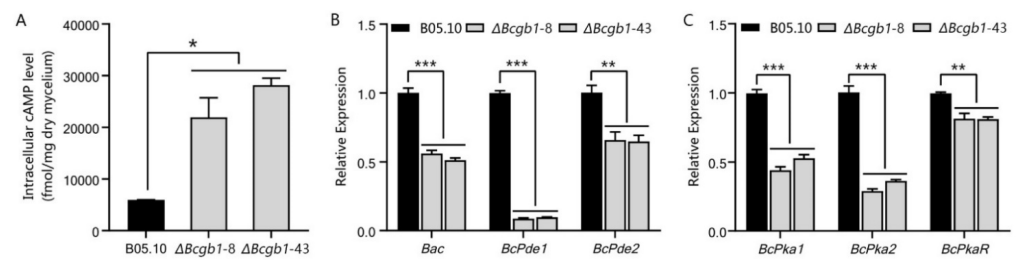


**Figure 5.** *Bcgb1* is involved in the regulation of intracellular cAMP levels. (A) Quantitative determination of intracellular cAMP levels in mycelia of the indicated strains cultured in PDB for 2 days. Two biological repetitions with three replicates were assayed. The error bars represent the SD of three replicates. (B) Transcript level of *Bac*, *BcPde1*, and *BcPde2* in the WT and the  $\Delta Bcgb1$  mutants of *B. cinerea*. (C) Transcript level of *BcPka1*, *BcPka2*, and *BcPkaR* in the WT and the  $\Delta Bcgb1$  mutants of *B. cinerea*. \*  $p < 0.05$ , \*\*  $p < 0.01$ , \*\*\*  $p < 0.001$ .

Due to the cAMP levels having increased in  $\Delta Bcgb1$  mutants, we further examined the transcript levels of the cAMP signaling pathway-related genes, such as the adenylate cyclase gene *Bac*, two phosphodiesterase genes (*BcPde1* and *BcPde2*), and three cAMP-dependent protein kinase (PKA) encoding genes (*BcPka1*, *BcPka2*, and *BcPkaR*). Interestingly, the expression of these six genes (*Bac*, *BcPde1*, *BcPde2*, *BcPka1*, *BcPka2*, and *BcPkaR*) was all significantly reduced in the  $\Delta Bcgb1$  mutants (Figure 5B,C). These results indicate that *Bcgb1* is required for maintaining normal cAMP levels in *B. cinerea*.

### 3.6. *Bcgb1* Plays an Important Role in Two MAPK (*Bmp1* and *Bmp3*) Signaling Pathways

To investigate whether *Bcgb1* plays a role in the MAPK (*Bmp1* and *Bmp3*) signaling pathway, we examined the phosphorylation levels of *Bmp1* and *Bmp3* in  $\Delta Bcgb1$  mutants with an anti-TpEY antibody. A Western blotting assay showed that  $\Delta Bcgb1$  mutants were increased in *Bmp1* and *Bmp3* phosphorylation compared with the wild type (Figure 6A). To further explore the role of *Bcgb1* in *Bmp1* and *Bmp3* phosphorylation, we examined the interaction of *Bcgb1* with the components of two MAPK signaling cascades (*BcSte11*/*BcSte7*/*Bmp1*, *BcBck1*/*BcMkk1*/*Bmp3*, and the MAPK adapter protein *BcSte50*). The results of yeast two-hybrid show that *Bcgb1* directly interacted with both *Bmp1* cascade protein (*BcSte11*) and *Bmp3* cascade proteins (*BcBck1* and *BcMkk1*). Moreover, *Bcgb1* directly interacted with the MAPK adapter protein *BcSte50* (Figure 6B).

To test whether deletion of *Bcgb1* altered expression of the downstream target genes of *Bmp1*, we measured the transcript level of a target gene, *Bcgas2* [16], in the  $\Delta Bcgb1$  mutants and wild type. The results of the qRT-PCR show that the *Bcgas2* transcript level was significantly increased in the  $\Delta Bcgb1$  mutants (Figure 6C). Our findings suggest that *Bcgb1* plays an important role in the MAPK (*Bmp1* and *Bmp3*) signaling pathway.

### 3.7. Deletion of *Bcgb1* Affects the Expression of Sclerotia Formation-Related Genes

Because  $\Delta Bcgb1$  mutants lost the ability to form sclerotia, we examined whether *Bcgb1* is involved in controlling the expression of sclerotia formation-related genes in *B. cinerea*. Twelve genes that were confirmed to be related to sclerotia formation were selected to detect the expression in the  $\Delta Bcgb1$  mutants and wild type by qRT-PCR (Figure 7). Three genes encoding the VELVET complex (*BcLaeA1*, *BcVEL1*, and *BcVEL2*) were differentially affected in the  $\Delta Bcgb1$  mutants. The expression of *BcLaeA1* in  $\Delta Bcgb1$  mutants was similar to that in wild type. However, in  $\Delta Bcgb1$  mutants, the transcript level of *BcVEL1* was down-regulated, whereas *BcVEL2* was up-regulated. The expression of two NADPH oxidases genes (*BcNoxA* and *BcNoxD*) was significantly reduced in  $\Delta Bcgb1$  mutants. Among six melanogenic genes, four genes (*Bcbrn2*, *Bcscd1*, *Bcsmr1*, and *BcPKS12*) were repressed in  $\Delta Bcgb1$  mutants. In contrast, other two melanogenic genes (*Bcbrn1* and *BcPKS13*) were overexpressed in  $\Delta Bcgb1$  mutants. Furthermore, expression of the bZIP transcription factor gene *BcAtf1*, which is required for sclerotia formation, was decreased in  $\Delta Bcgb1$  mutants.

Taken together, the expression studies suggested that Bcgb1 plays an important role in regulation of sclerotia formation-related gene expression in *B. cinerea*.

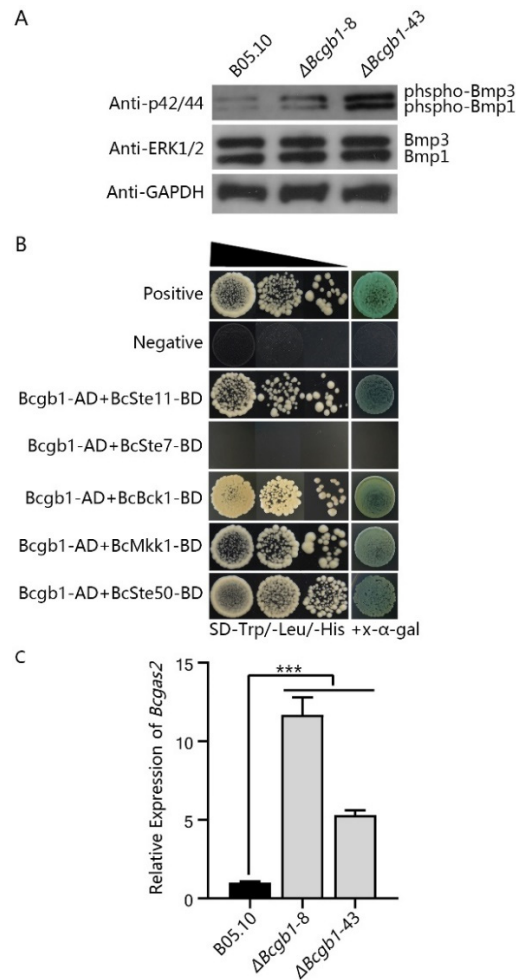


**Figure 6.** Bcgb1 negatively regulates the Bmp1 and Bmp3 MAPK pathway in *B. cinerea*. **(A)** Phosphorylation level of MAPK (Bmp1 and Bmp3) in the  $\Delta Bcgb1$  mutants. Bmp1 and Bmp3 and their phosphorylated proteins were detected using the ERK1/2 and phospho-p44/42 MAPK antibodies, respectively. The intensity of the phosphorylated Bmp1 and Bmp3 band for each strain is relative to that of the Bmp1 and Bmp3 band, respectively. **(B)** Yeast two-hybrid assay between Bcgb1 and BcSte11/BcSte7/Bmp1 and BcBck1/BcMkk1/Bmp3 cassette. The pGBKT7-53 and pGADT7-T pair of plasmids served as the positive control. The pGBKT7-Lam and pGADT7-T pair of plasmids served as the negative control. Yeast cells were drop-plated on SD-Trp/-Leu/-His with x- $\alpha$ -gal. **(C)** Transcript level of the Bmp1 MAPK-regulated gene *Bcgas2* in the WT and the  $\Delta Bcgb1$  mutants of *B. cinerea*. \*\*\*  $p < 0.001$ .

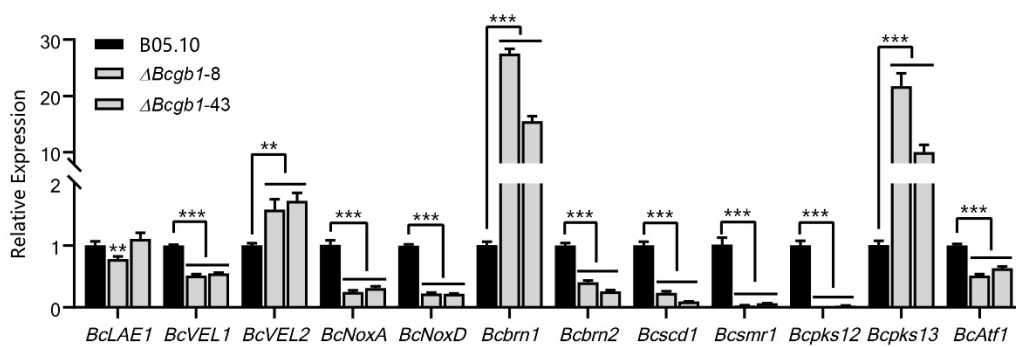


**Figure 7.** Transcript level of the sclerotia formation-related genes in the WT and the  $\Delta Bcgb1$  mutants of *B. cinerea*. \*\*  $p < 0.01$ , \*\*\*  $p < 0.001$ .

#### 4. Discussion

In this study, we characterized the function of the G $\beta$  gene *Bcgb1* in *B. cinerea*, which revealed the multifaceted roles of *Bcgb1* in development and virulence. To date, the functions of the G $\beta$  gene have already been studied in several plant pathogenic fungi, including *C. parasitica* [24], *M. grisea* [7], *F. oxysporum* [9], *Ustilago maydis* [25], *Cochliobolus heterostrophus* [26], *F. verticillioides* [27], *Gibberella zeae* [28], and *V. dahliae* [12]. Interestingly, the G $\beta$  gene in plant pathogenic fungi played varying roles in development and pathogenicity.

Loss of *Bcgb1* in *B. cinerea* caused mutants with a significant decrease in virulence. This is consistent with the function of the G $\beta$  gene in most plant pathogenic fungi, except that the G $\beta$  gene deletion mutants showed a slightly reduced in virulence in *U. maydis* [25] and *F. verticillioides* [27]. In *B. cinerea*, an infection cushion is a special infection structure that is necessary for successful infection of mycelia. The  $\Delta Bcgb1$  mutant was defective in infection cushion formation, and was responsible for reduced virulence. Similarly, the G $\beta$  gene played a critical role in the infection structure (appressorium) formation and pathogenicity in *M. grisea* [7] and *C. heterostrophus* [26].

Deletion of *Bcgb1* resulted in altered colony morphology and decreased mycelial growth rate, but increased aerial hyphae and mycelia biomass. Alteration of colony morphology was also presented in the G $\beta$  deletion mutant of *F. oxysporum* [9] and *V. dahliae* [12]. In *Aspergillus nidulans*, the G $\beta$  deletion mutant  $\Delta sfaD$  showed a significant reduction in mycelial mass, although the growth rate was similar to wild type [29]. Similar to the  $\Delta Bcgb1$  mutant, more aerial hyphae were also found in the G $\beta$  mutant of *M. grisea* [7]. In contrast, the G $\beta$  gene *cpgb-1* was required for normal aerial hyphae formation in the chestnut blight fungus *C. parasitica* [24]. In *F. verticillioides*, the G $\beta$  gene *gbb1* was dispensable for mycelial growth and mycelial mass but important for mycotoxin fumonisin B<sub>1</sub> production [27]. These results indicate that G $\beta$  in filamentous fungi plays different roles in mycelial growth.

The G $\beta$  gene is required for sporulation in *B. cinerea*, which was also found in several fungi, such as *C. parasitica* [24], *M. grisea* [7], *F. oxysporum* [9], *C. heterostrophus* [26], and *F. verticillioides* [26]. However, the opposite results, that deletion of G $\beta$  gene caused increased conidiation, were observed in *A. nidulans* [29] and *V. dahliae* [12]. In addition, the  $\Delta Bcgb1$  mutants failed to form sclerotia, but the G $\beta$  mutants of *V. dahliae* enhanced sclerotia formation [12]. It is suggested that the role of G $\beta$  in conidiation and sclerotia formation was opposite in *B. cinerea* and *V. dahliae*. The qRT-PCR results revealed that loss of G $\beta$  affected the expression of sclerotia formation-related genes, indicating that G $\beta$  is an upstream regulatory component of these genes.

In filamentous fungi, G proteins are involved in the regulation of cAMP signaling that controls multiple cellular processes, including growth, development, and virulence [4]. Deletion of the G $\beta$  gene resulted in reduced intracellular cAMP levels in *N. crassa* [30], *M. grisea* [7], and *F. oxysporum* [9]. In addition, loss of G $\beta$  caused a decreased in G $\alpha$  protein levels in *C. parasitica* [31] and *N. crassa* [30]. Therefore, G $\beta$  should maintain normal levels of G $\alpha$  protein, which stimulates adenylate cyclase activity to form cAMP [32]. However, the intracellular cAMP levels were drastically increased in  $\Delta Bcgb1$  mutants (Figure 5A),

indicating that G $\beta$  serves as an inhibitor to suppress the activity of G $\alpha$  proteins in *B. cinerea*. The adenylate cyclase (cAMP biosynthesis) and phosphodiesterase (cAMP hydrolysis) are crucial regulators for maintaining the balance of intracellular cAMP levels [33]. In this study, expression of adenylate cyclases gene (*Bac*) and phosphodiesterases genes (*BcPde1* and *BcPde2*) was significantly reduced in the  $\Delta Bcgb1$  mutants (Figure 5B). The possible explanation is that *Bcgb1* deletion inhibits the transcription of *BcPde1* and *BcPde2*, resulting in increased cAMP levels that may feedback suppress the expression of *Bac*. Thus, the activities of adenylate cyclase and phosphodiesterase in  $\Delta Bcgb1$  mutants needs to be further investigated. Another cAMP signaling component is the cAMP-dependent protein kinase (PKA), consisting of two regulatory subunits and two catalytic subunits. In *B. cinerea*, BcPka1 and BcPka2 belong to a catalytic subunit, and BcPkaR is the regulatory subunit [34]. Deletion mutants of PKA ( $\Delta BcPka1$ ,  $\Delta BcPka2$ , and  $\Delta BcPkaR$ ) all showed significantly increased intracellular cAMP levels in mycelia, suggesting that the PKA (BcPka1, BcPka2, and BcPkaR) negatively regulates the intracellular cAMP levels in *B. cinerea* [34]. Similarly, a significant reduction in expression of three PKA genes (*BcPka1*, *BcPka2*, and *BcPkaR*) and increased intracellular cAMP levels were also observed in  $\Delta Bcgb1$  mutants (Figure 5C).

In *Saccharomyces cerevisiae* yeast, the G $\beta$  protein Ste4p is required to transfer the pheromone signal to activate the MAPK mating pathway [35]. However, deletion of G $\beta$  gene *fgb1* did not affect phosphorylation level of the MAP kinase Fmk1 in *F. oxysporum* [31]. Our results show that phosphorylation levels of MAP kinases (Bmp1 and Bmp3) were increased in  $\Delta Bcgb1$  mutants (Figure 6A), supporting the hypothesis that G $\beta$  regulates the MAPK signaling pathway downstream in *Cryptococcus neoformans* [36] and *M. grisea* [7]. Yeast two-hybrid assays showed that G $\beta$  protein Bcgb1 directly interacted with MAPK cascade proteins (BcSte11, BcBck1, BcMkk1, and BcSte50) (Figure 6B). This provides evidence that G $\beta$  is involved in the MAPK signaling pathway. Additional evidence is that *Bcgas2*, the downstream regulated gene of Bmp1 [16], was up-regulated in the  $\Delta Bcgb1$  mutant. These results suggest that G $\beta$  protein Bcgb1 plays an important role in the regulation of the MAPK signaling pathway in *B. cinerea*.

Previous studies have demonstrated that deletion of the MAP kinase Bmp1 causes defects in conidia germination, reduces mycelial growth, causes a failure to form sclerotia, and induces a loss of pathogenicity in *B. cinerea* [37]. Another MAP kinase, Bmp3, is important for growth, conidiation, sclerotia formation, and virulence [38]. Interestingly, the  $\Delta Bcgb1$  mutants showed similar defective phenotypes, but increased phosphorylation levels of Bmp1 and Bmp3. Maintenance of normal phosphorylation levels of MAPK is critical for the MAPK signaling pathway in eukaryotic cells. Our data indicate that G $\beta$  protein Bcgb1 is required for maintaining normal phosphorylation levels of Bmp1 and Bmp3 in *B. cinerea*.

In conclusion, this study presents evidence that Bcgb1 not only plays an important role in the cAMP signaling pathway, but also regulates the MAPK signaling pathway. Bcgb1 may function in cross-talks between these signaling pathways. This might explain the defects of the  $\Delta Bcgb1$  mutant in mycelial growth, conidiation, sclerotia formation, and virulence. These data provide new insight into the multiple functions of the G $\beta$  protein in filamentous fungi. Further studies are necessary to reveal the molecular mechanism of G $\beta$  in regulating the cAMP signaling pathway and MAPK signaling pathway.

**Supplementary Materials:** The following are available online at <https://www.mdpi.com/article/10.3390/jof7060431/s1>, Figure S1: Disruption of *Bcgb1* in *B. cinerea*: (A) Schematic diagram indicating the strategy for disruption of *Bcgb1* by the homologous recombination event in *B. cinerea*. *HPT*, hygromycin phosphate transferase gene, (B) PCR confirmation of disruption of the *Bcgb1* gene in different mutants of *B. cinerea*, and (C) Southern blot confirmation of the disruption of *Bcgb1*; Table S1: Primers used in this study.

**Author Contributions:** Conceptualization, J.T. and L.Y.; methodology, J.T., M.W., and J.Z.; software, J.T.; validation, J.T.; formal analysis, J.T. and L.Y.; investigation, J.T. and L.Y.; resources, G.L. and L.Y.;

data curation, J.T. and L.Y.; writing—original draft preparation, J.T.; writing—review and editing, G.L. and L.Y.; supervision, G.L. and L.Y.; project administration, M.W., J.Z., and L.Y.; funding acquisition, L.Y. All authors have read and agreed to the published version of the manuscript.

**Funding:** This research was funded by the Fundamental Research Funds for the Central Universities (grant no. 2662020ZKPY010).

**Institutional Review Board Statement:** Not applicable.

**Informed Consent Statement:** Not applicable.

**Data Availability Statement:** Not applicable.

**Acknowledgments:** The authors thank Guotian Li (Huazhong Agricultural University) for his kind suggestions.

**Conflicts of Interest:** The authors declare no conflict of interest.

## References

- Elad, Y.; Pertot, I.; Prado, A.M.C.; Stewart, A. Plant hosts of *Botrytis* spp. In *Botrytis—the Fungus, the Pathogen and Its Management in Agricultural Systems*; Fillinger, S., Elad, Y., Eds.; Springer: Berlin/Heidelberg, Germany, 2016; p. 6.
- Dean, R.; van Kan, J.A.L.; Pretorius, Z.A.; Hammond-Kosack, K.E.; di Pietro, A.; Spanu, P.D.; Rudd, J.J.; Dickman, M.; Kahmann, R.; Ellis, J.; et al. The top 10 fungal pathogens in molecular plant pathology. *Mol. Plant Pathol.* **2012**, *13*, 414–430. [[CrossRef](#)] [[PubMed](#)]
- Carisse, O. Epidemiology and aerobiology of *Botrytis* spp. In *Botrytis—the Fungus, the Pathogen and Its Management in Agricultural Systems*; Fillinger, S., Elad, Y., Eds.; Springer: Berlin/Heidelberg, Germany, 2016; p. 133.
- Li, L.; Wright, S.J.; Krystofova, S.; Park, G.; Borkovich, K.A. Heterotrimeric G protein signaling in filamentous fungi. *Annu. Rev. Microbiol.* **2007**, *61*, 423–452. [[CrossRef](#)] [[PubMed](#)]
- Cabrera-Vera, T.M.; Vanhauwe, J.; Thomas, T.O.; Medkova, M.; Preininger, A.; Mazzoni, M.R.; Hamm, H.E. Insights into G protein structure, function, and regulation. *Endocr. Rev.* **2003**, *24*, 765–781. [[CrossRef](#)] [[PubMed](#)]
- Liu, S.; Dean, R.A. G protein alpha subunit genes control growth, development, and pathogenicity of *Magnaporthe grisea*. *Mol. Plant Microbe Interact.* **1997**, *10*, 1075–1086. [[CrossRef](#)]
- Nishimura, M.; Park, G.; Xu, J.R. The G-beta subunit MGB1 is involved in regulating multiple steps of infection-related morphogenesis in *Magnaporthe grisea*. *Mol. Microbiol.* **2003**, *50*, 231–243. [[CrossRef](#)]
- Li, Y.; Que, Y.; Liu, Y.; Yue, X.; Meng, X.; Zhang, Z.; Wang, Z. The putative G $\gamma$  subunit gene MGG1 is required for conidiation, appressorium formation, mating and pathogenicity in *Magnaporthe oryzae*. *Curr. Genet.* **2015**, *61*, 641–651. [[CrossRef](#)]
- Jain, S.; Akiyama, K.; Kan, T.; Ohguchi, T.; Takata, R. The G protein beta subunit FGB1 regulates development and pathogenicity in *Fusarium oxysporum*. *Curr. Genet.* **2003**, *43*, 79–86. [[CrossRef](#)]
- Jain, S.; Akiyama, K.; Mae, K.; Ohguchi, T.; Takata, R. Targeted disruption of a G protein alpha subunit gene results in reduced pathogenicity in *Fusarium oxysporum*. *Curr. Genet.* **2002**, *41*, 407–413. [[CrossRef](#)]
- Jain, S.; Akiyama, K.; Takata, R.; Ohguchi, T. Signaling via the G protein a subunit FGA2 is necessary for pathogenesis in *Fusarium oxysporum*. *FEMS Microbiol. Lett.* **2005**, *243*, 165–172. [[CrossRef](#)]
- Tzima, A.K.; Paplomatas, E.J.; Tsitsigiannis, D.I.; Kang, S. The G protein  $\beta$  subunit controls virulence and multiple growth- and development-related traits in *Verticillium dahliae*. *Fungal Genet. Biol.* **2012**, *49*, 271–283. [[CrossRef](#)]
- Gronover, C.S.; Kasulke, D.; Tudzynski, P. The role of G protein alpha subunits in the infection process of *Botrytis cinerea*. *Mol. Plant Microbe Interact.* **2001**, *14*, 1293–1302. [[CrossRef](#)]
- Gronover, C.S.; Schorn, C.; Tudzynski, B. Identification of *Botrytis cinerea* genes up-regulated during infection and controlled by the G alpha subunit BCG1 using suppression subtractive hybridization (SSH). *Mol. Plant Microbe Interact.* **2004**, *17*, 537–546. [[CrossRef](#)]
- Döhlemann, G.; Berndt, P.; Hahn, M. Different signaling pathways involving a G alpha protein, cAMP and a MAP kinase control germination of *Botrytis cinerea* conidia. *Mol. Microbiol.* **2006**, *59*, 821–836. [[CrossRef](#)] [[PubMed](#)]
- Schamber, A.; Lerach, M.; Diwo, J.; Mendgen, K.; Hahn, M. The role of mitogen-activated protein (MAP) kinase signalling components and the Ste12 transcription factor in germination and pathogenicity of *Botrytis cinerea*. *Mol. Plant Pathol.* **2010**, *11*, 105–119. [[CrossRef](#)] [[PubMed](#)]
- Lou, Y.; Han, Y.; Yang, L.; Wu, M.; Zhang, J.; Cheng, J.; Wang, M.; Jiang, D.; Chen, W.; Li, G. CmpacC regulates mycoparasitism, oxalate degradation and antifungal activity in the mycoparasitic fungus *Coniothyrium minitans*. *Environ. Microbiol.* **2015**, *17*, 4711–4729. [[CrossRef](#)]
- Kershaw, M.J.; Talbot, N.J. Genome-wide functional analysis reveals that infection-associated fungal autophagy is necessary for rice blast disease. *Proc. Natl. Acad. Sci. USA* **2009**, *106*, 15967–15972. [[CrossRef](#)] [[PubMed](#)]
- Liu, X.; Xie, J.; Fu, Y.; Jiang, D.; Chen, T.; Cheng, J. The subtilisin-like protease Bcser2 affects the sclerotial formation, conidiation and virulence of *Botrytis cinerea*. *Int. J. Mol. Sci.* **2020**, *21*, 603. [[CrossRef](#)]

20. Zeng, L.M.; Zhang, J.; Han, Y.C.; Yang, L.; Wu, M.D.; Jiang, D.H.; Chen, W.; Li, G.Q. Degradation of oxalic acid by the mycoparasite *Coniothyrium minitans* plays an important role in interacting with *Sclerotinia sclerotiorum*. *Environ. Microbiol.* **2014**, *16*, 2591–2610. [[CrossRef](#)]
21. Zhang, L.; Wu, M.D.; Li, G.Q.; Jiang, D.H.; Huang, H.C. Effect of Mitovirus infection on formation of infection cushions and virulence of *Botrytis cinerea*. *Physiol. Mol. Plant Pathol.* **2010**, *75*, 71–80. [[CrossRef](#)]
22. Xu, Y.; Wang, Y.; Zhao, H.; Wu, M.; Zhang, J.; Chen, W.; Li, G.; Yang, L. Genome-wide identification and expression analysis of the bZIP transcription factors in the mycoparasite *Coniothyrium minitans*. *Microorganisms* **2020**, *8*, 1045. [[CrossRef](#)] [[PubMed](#)]
23. Zhang, X.; Bian, Z.; Xu, J.R. Assays for MAP kinase activation in *Magnaporthe oryzae* and other plant pathogenic fungi. In *Plant Pathogenic Fungi and Oomycetes; Methods in Molecular Biology*; Ma, W., Wolpert, T., Eds.; Humana: New York, NY, USA, 2018; Volume 1848. [[CrossRef](#)]
24. Kasahara, S.; Nuss, D.L. Targeted disruption of a fungal G-protein  $\beta$  subunit gene results in increased vegetative growth but reduced virulence. *Mol. Plant Microbe Interact.* **1997**, *10*, 984–993. [[CrossRef](#)] [[PubMed](#)]
25. Müller, P.; Leibbrandt, A.; Teunissen, H.; Cubasch, S.; Aichinger, C.; Kahmann, R. The G $\beta$ -subunit-encoding gene *bpp1* controls cyclic-AMP signaling in *Ustilago maydis*. *Eukaryot. Cell* **2004**, *3*, 806–814. [[CrossRef](#)] [[PubMed](#)]
26. Ganem, S.; Lu, S.W.; Lee, B.N.; Chou, D.Y.T.; Hadar, R.; Turgeon, B.G.; Horwitz, B.A. G-protein  $\beta$  subunit of *Cochliobolus heterostrophus* involved in virulence, asexual and sexual reproductive ability, and morphogenesis. *Eukaryot. Cell* **2004**, *3*, 1653–1663. [[CrossRef](#)]
27. Sagaram, U.S.; Shim, W.B. *Fusarium verticillioides* *GBB1*, a gene encoding heterotrimeric G protein  $\beta$  subunit, is associated with fumonisin B<sub>1</sub> biosynthesis and hyphal development but not with fungal virulence. *Mol. Plant Pathol.* **2007**, *8*, 375–384. [[CrossRef](#)] [[PubMed](#)]
28. Yu, H.Y.; Seo, J.A.; Kim, J.E.; Han, K.H.; Shim, W.B.; Yun, S.H.; Lee, Y.W. Functional analyses of heterotrimeric G protein G alpha and G beta subunits in *Gibberella zeae*. *Microbiology* **2008**, *154*, 392–401. [[CrossRef](#)]
29. Rosén, S.; Yu, J.H.; Adams, T.H. The *Aspergillus nidulans* *sfaD* gene encodes a G protein  $\beta$  subunit that is required for normal growth and repression of sporulation. *EMBO J.* **1999**, *18*, 5592–5600. [[CrossRef](#)]
30. Yang, Q.; Poole, S.I.; Borkovich, K.A. A G-protein beta subunit required for sexual and vegetative development and maintenance of normal G alpha protein levels in *Neurospora crassa*. *Eukaryot. Cell* **2002**, *1*, 378–390. [[CrossRef](#)]
31. Kasahara, S.; Wang, P.; Nuss, D.L. Identification of *bdm-1*, a gene involved in G protein  $\beta$ -subunit function and  $\alpha$ -subunit accumulation. *Proc. Natl. Acad. Sci. USA* **2000**, *97*, 412–417. [[CrossRef](#)]
32. Delgado-Jarana, J.; Martínez-Rocha, A.L.; Roldán-Rodríguez, R.; Roncero, M.I.G.; Di Pietro, A. *Fusarium oxysporum* G-protein subunit *Fgb1* regulates hyphal growth, development, and virulence through multiple signaling pathways. *Fungal Genet. Biol.* **2005**, *42*, 61–72. [[CrossRef](#)]
33. Sassone-Corsi, P. The cyclic AMP pathway. *Cold Spring Harb. Perspect. Biol.* **2012**, *4*, a011148. [[CrossRef](#)]
34. Schumacher, J.; Kokkelink, L.; Huesmann, C.; Jimenez-Teja, D.; Collado, I.G.; Barakat, R.; Tudzynski, P.; Tudzynski, B. The cAMP-dependent signaling pathway and its role in conidial germination, growth, and virulence of the gray mold *Botrytis cinerea*. *Mol. Plant Microbe Interact.* **2008**, *21*, 1443–1459. [[CrossRef](#)]
35. Hoffman, C.S. Except in every detail: Comparing and contrasting G-protein signaling in *Saccharomyces cerevisiae* and *Schizosaccharomyces pombe*. *Eukaryot. Cell* **2005**, *4*, 495–503. [[CrossRef](#)]
36. Wang, P.; Perfect, J.R.; Heitman, J. The G-protein beta subunit *GPB1* is required for mating and haploid fruiting in *Cryptococcus neoformans*. *Mol. Cell. Biol.* **2000**, *20*, 352–362. [[CrossRef](#)] [[PubMed](#)]
37. Zheng, L.; Campbell, M.; Murphy, J.; Lam, S.; Xu, J.R. The *BMP1* gene is essential for pathogenicity in the gray mold fungus *Botrytis cinerea*. *Mol. Plant Microbe Interact.* **2000**, *13*, 724–732. [[CrossRef](#)] [[PubMed](#)]
38. Rui, O.; Hahn, M. The Slr2-type MAP kinase *Bmp3* of *Botrytis cinerea* is required for normal saprotrophic growth, conidiation, plant surface sensing and host tissue colonization. *Mol. Plant Pathol.* **2007**, *8*, 173–184. [[CrossRef](#)] [[PubMed](#)]